Journal of Sol-Gel Science and Technology 29, 97–105, 2004

Sol-Gel Derived Nanocomposites and Nanoporous Oxide Powders and Related Coatings for the Reversible Chemisorption of Hydrogen Sulfide

R.L. GOSWAMEE
Material Science Division, Regional Research Laboratory, Jorhat, 785006, Assam, India

F. BOSC, D. COT, A. EL MANSOURI AND M. LOPEZ
Institut Européen des Membranes, UMR CNRS 5635, CC 47, Université Montpellier II, Place Eugène Bataillon, 34095 Montpellier cedex 5, France

F. MORATO
Laboratoire des Agrégats Moléculaires et Matériaux Inorganiques, UMR CNRS 5072, CC 4, Université Montpellier II, Place Eugène Bataillon, 34095 Montpellier cedex 5, France

A. AYRAL*
Institut Européen des Membranes, UMR CNRS 5635, CC 47, Université Montpellier II, Place Eugène Bataillon, 34095 Montpellier cedex 5, France
Andre.Ayral@iemm.univ-montp2.fr

Received June 19, 2003; Accepted December 24, 2003

Abstract. Two types of nanocomposites and nanoporous powders and related coatings were prepared by the sol-gel route. These silica-based materials contain dispersed reactive oxides, ZnO and $ZnCr_2O_4$, respectively. Experiments evidenced their ability of reversible chemisorption of H_2S as ZnS. Their attractive porous characteristics (small pore size ∼2–2.5 nm, high specific surface area ∼900–1100 $m^2 \cdot g^{-1}$, high porosity ∼50–60%) are not significantly modified during the successive treatments of H_2S chemisorption and oxide regeneration. These preliminary results encourage to pursue this study which aims at the preparation of nanofilters for the desulfurization of gas mixtures.

Keywords: silica-based nanocomposites, reversible H_2S chemisorption, nanoporous materials

1. Introduction

Single or mixed reactive oxides can be used for removing toxic gas from gas mixtures by catalytic conversion or selective adsorption [1–4]. For instance, a compound like hydrogen sulfide, H_2S, which is present in natural gas has to be removed because is a severe poison for the reforming catalysts. Iron oxide was previously used for chemisorbing H_2S as FeS. Iron oxide is however not enough efficient for desulfurizing the feed to a steam reformer [2] and it suffers also from the disadvantage that the reaction is rapid and exothermic and potentially hazardous in the presence of a combustible gas [3]. It is now usually replaced by zinc oxide [2, 3] leading to the reversible transition into ZnS. It has been previously shown that a complex oxide like zinc chromite, $ZnCr_2O_4$, can also reversibly chemsorb hydrogen sulfide [4].

*To whom all correspondence should be addressed.

In addition to the design of the solid-gas contactor device, the yield of a desulfurization process directly depends on the physicochemical properties of the used adsorbent : crystallite size of the active phase, specific surface area, porous texture. In the case of a microporous solid (pore size less than 2 nm), if the gas flow is forced across the microporosity, it can be expected that the retention will be highly efficient. As a matter of fact, the probability for a gas molecule to interact with the active walls of the adsorbent will be close to 1. This situation could be reached with the preparation of active nanofilters like supported microporous membranes. The lower gas permeability of such microporous barriers is counterbalanced by the thinness of the active layer which limits the energy-consuming pressure loss [5]. In return, the low amount of adsorbent restricts the potential applications to the elimination of traces in high-purity gas or to the design of integrated filters for miniaturized devices like micro fuel cells.

This work is a first contribution to a feasibility study of such active nanofilters dedicated to the retention of hydrogen sulfide. These preliminary experiments are based on our know-how in the sol-gel preparation of nanoporous silica membranes [6]. Nanoporous silica was used as host matrix for reactive oxides, ZnO and $ZnCr_2O_4$. Powders and coatings were prepared and characterized.

2. Experimental

2.1. Materials

The selected metallic salts of Zn_{II} and Cr_{III} were hydrated nitrates, $Zn(NO_3)_2, 6H_2O$ and $Cr(NO_3)_3, 9H_2O$, respectively. They were first dissolved in ethanol under magnetic stirring (maintained until the end of the sol preparation). The silica precursor was tetraethoxysilane (TEOS), which was added to the alcoholic solutions. In the case of the samples containing only Zn_{II} (label SZ), the molar ratio of Si to Zn was 1:0.05. In the case of the samples containing both Zn_{II} and Cr_{III} (label SZC), the molar ratios of Si to Zn and to Cr were 1:0.05 and 1:0.1, respectively. Acidic water (0.2 $mol \cdot L^{-1}$ HCl) was then added according to a hydrolysis ratio (H_2O/Si) equal to 2. After an aging time of 45 min, basic water (0.2 $mol \cdot L^{-1}$ NH_3) was added to promote silica polycondensation. The final hydrolysis ratio was equal to 9. Immediately after the addition of basic water, an organic additive acting as porogen and filmogen agent was poured in the mixture. The selected additive was a non-ionic surfactant of octylphenyl polyether alcohol type (Triton X45, Fluka) [6]. Two molar ratios of Si to X45 were investigated, 4:1 and 2:1, respectively. After 5 min under stirring, the resulting sols were deposited by slip-casting (contact time: 5 min, drain rate: 10 $cm \cdot min^{-1}$) on commercial porous tubular alumina supports (Pall, Exekia Division). These substrates consisted of a 1 mm-thick tube of α-alumina with a mean pore size equal to 10 μm and successive layers deposited on the internal side with decreasing mean pore sizes: 0.8 μm, 0.2 μm and 5 nm for the γ-alumina top-layer. The residual solutions were poured in large beakers to provide powders equivalent to the previously deposited coatings.

After drying for 24 h at room temperature, the coatings and the powders were dried for 2 h at 100°C in an oven. The dried samples were then calcined using the following conditions: heating rate up to 220°C: 1°C/min; dwell at 220°C for 45 min; heating rate up to 550°C: 5°C/min; dwell at 550°C for 45 min. This thermal treatment was applied for removing the organic additive and for reinforcing the oxide network. The resulting samples will be later labeled SZx-A and SZCx-A, respectively, with $x = 2$ or 4, the value of the molar ratio Si:X45.

Reaction of powders SZ4-A and SZC4-A with H_2S were carried out inside a tubular furnace. Initially the calcined powders were heated at 500°C under N_2 for two hours. Pure H_2S was then passed over the adsorbent at 500°C for 3 h. After this the temperature brought down to 250°C under H_2S flow. Final cooling of the adsorbent was carried out under N_2 flow. The samples will be later labeled SZ4-B et SZC4-B, respectively. Oxide regeneration was performed under air up to 500°C (heating rate: 5°C/min). The samples heated for 90 min and for 180 min at 500°C will be labeled SZ4-C1 or SZC4-C1 and SZ4-C2 or SZC4-C2, respectively.

In addition, powder SZ4-A was thermally treated under air up to 750°C for 1 h (sample SZ4-D) and then up to 900°C for 1 h (sample SZ4-E).

2.2. Characterization

The morphology and the chemical analysis of the coatings deposited on the porous substrates were investigated using a scanning electron microscope (SEM) equipped with an Energy Dispersive Spectroscopy (EDS) device. The porosity of the powders was

characterized from the nitrogen adsorption-desorption isotherms at 77 K. The specific surface area, S_{BET}, and the micropore size distribution were determined using the BET and MP (micropore analysis) methods, respectively [7]. The mean pore size, d_p, was calculated assuming cylindrical pores and using the following equation: $d_p = 4\ V_p/S_{BET}$, where V_p is the pore volume determined from the N_2 adsorbed volume for a relative pressure of nitrogen close to 1. Thermogravimetric measurements were carried out on sample SZ4-B with heating rates ranging from 2 to 5°C/min. The structure of the crystalline phases was determined from X-ray patterns recorded with a diffractometer using a $\theta/2\theta$ Bragg-Brentano scattering geometry and the Cu-$L3,2$ radiation. Infrared spectra in the range 4000–400 cm^{-1} were recorded using a FTIR spectrometer and KBr pellets. Preliminary X-ray absorption spectroscopy measurements were performed at the Zn-K edge with an apparatus using a conventional X-ray tube with a molybdenum anti-cathode as X-ray source and a germanium monochromator [8].

3. Results and Discussion

3.1. Coatings on Porous Substrates

SEM images and related EDS spectra of different coatings are shown in Fig. 1. In the case of samples prepared with the lowest additive content (SZ4 and SZC4), it is difficult to clearly detect the presence of a thin layer on the mesoporous top layer of the substrate. On the other hand, the SEM observations evidence a complete infiltration of this top layer by the deposited sol and an extension of the infiltration to the intermediate layers of the substrate. In the case of samples with the highest additive content (SZ2 et SZC2), the higher viscosity

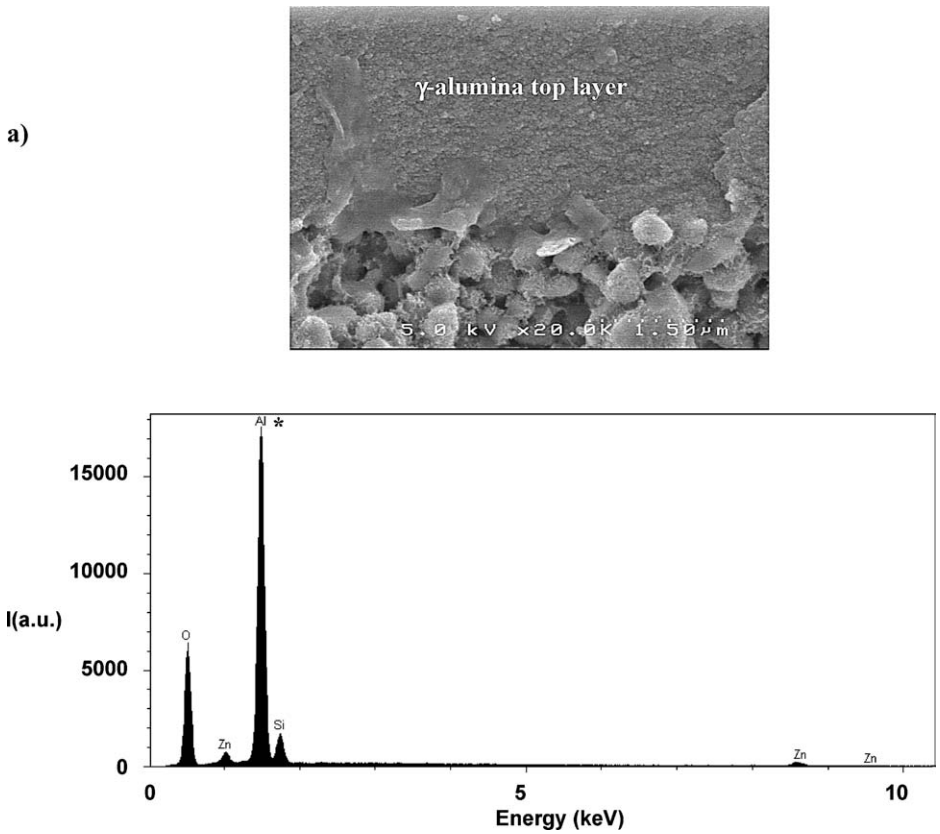

Figure 1. SEM cross-section images of coatings on porous alumina substrates and related EDS spectra from the coating surface, (a) SZ4-A and (b) SZC2-A. (*: peak of Al due to the alumina substrate).

(*Continued on next page*.)

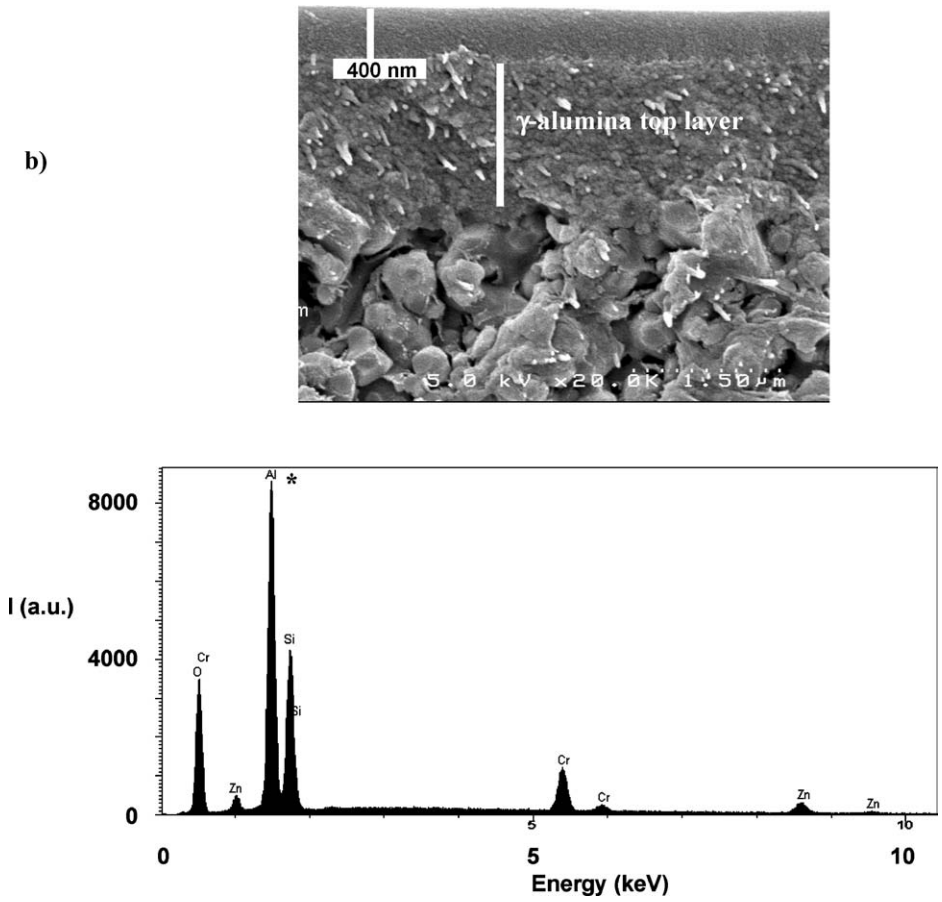

Figure 1. (*Continued*).

of the deposited sol leads to few 100 nm-thick films. The infiltration is limited and essentially concerns the mesoporous top layer of the substrate. Considering the previously discussed application as gas nanofilters, the infiltration of the top layer of the substrate is not a severe problem in term of pressure loss. Moreover this type of composite membrane obtained by filling the porosity of the substrate minimizes the risks of major defects in the filtering barrier. On the other hand, an increase of the additive content is still possible without significant variation of the pore size in the coating [6].

3.2. Structural Evolution and Study of the Sulfurization-Desulfurization Process

The X-ray pattern of powder SZ4-A is given in Fig. 2. This material is amorphous without any detectable presence of ZnO nanocrystallites. The corresponding IR spectrum is identical to that of amorphous silica synthesized with the same conditions. No significant modification is in particular visible in the range of absorption of ZnO, between 600 et 400 cm^{-1} [9]. Preliminary X-ray absorption spectroscopy measurements were performed on this sample. No pre-edge peak or white line is observed on the expanded X-ray absorption spectrum and no oscillation appear in the EXAFS region. It can be concluded that the zinc atoms do not exhibit a specific environment and appear as homogeneously dispersed in the silica matrix. At this stage, the synthesized material is a ZnO-doped silica rather than a nanocomposite material since ZnO segregation is not experimentally evidenced. These results are in good agreement with the X-ray diffraction analyses performed on samples heated at higher temperature (Fig. 3). At 750°C, sample SZ4-D remains amorphous whereas at 900°C, diffraction peaks are detected which can be associated with the presence of the intermediate compound Zn_2SiO_4 [10] found in the ZnO-SiO_2

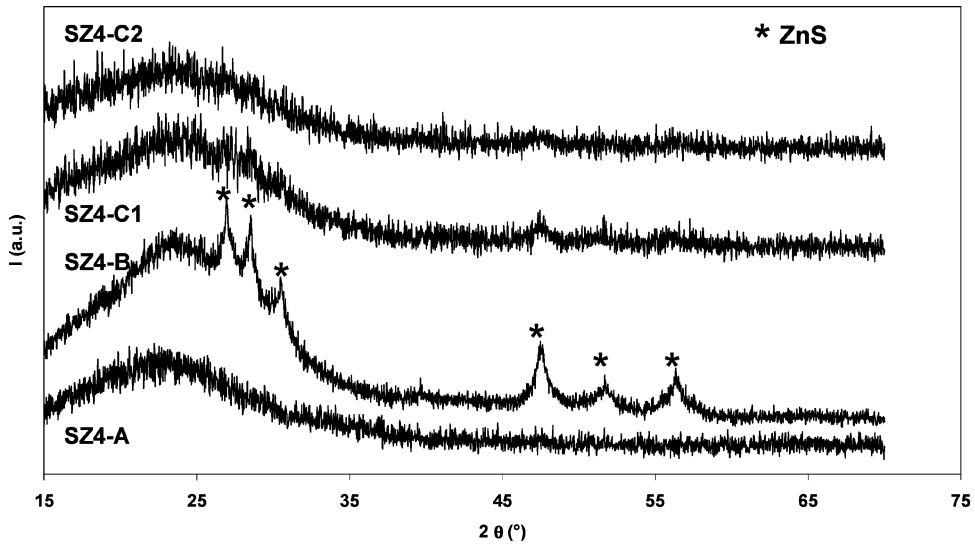

Figure 2. X-ray patterns for different samples SZ4.

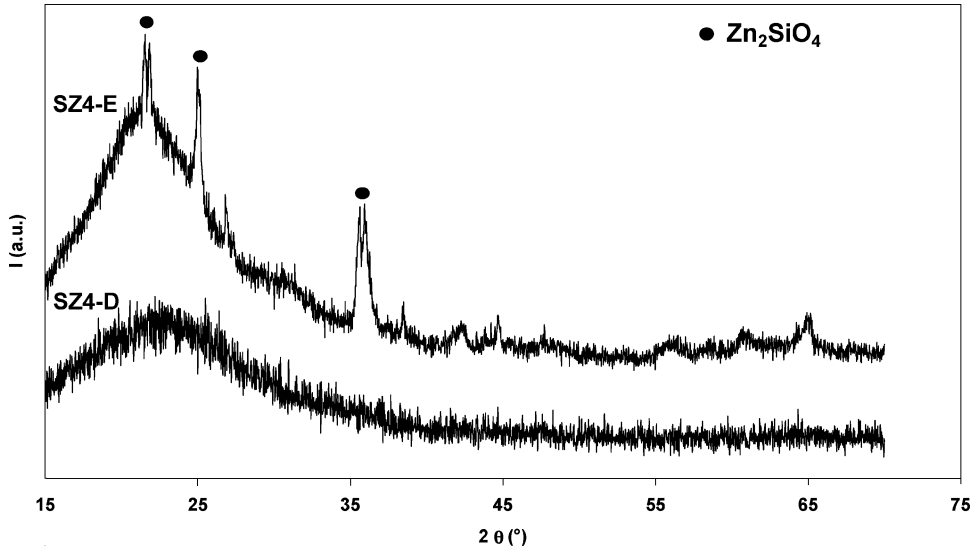

Figure 3. X-ray patterns for samples SZ4-D and SZ4-E.

binary diagram [11]. After thermal treatment under H_2S, broad peaks related to the presence of nanocrystallites of ZnS würzite [12] appear on the X-ray pattern of powder SZ4-B (Fig. 2). The regeneration treatment under air induces the progressive decrease of the intensity of the peaks of ZnS. For 180 min at 500°C (sample SZ4-C2—Fig. 2), the quasi-complete disappearance of these diffraction peaks leads to a pattern similar to that of sample SZ4-A. This result indicates the reversibility of the chemisorption of H_2S as ZnS. This phenomenon can be explained by the homogeneous dispersion at the nanometer scale of the zinc cations in the silica matrix associated with their high mobility enabling germination and growth of ZnS nuclei. We tried to quantify the yield of sulfurization from thermogravimetric analyses on sample SZ4-B. Assuming a complete sulfurization of all the zinc atoms, it was expected a theoretical weight loss of 1.2% due to the transition from ZnS to ZnO. Experimentally a continuous weight loss of ∼5% is observed between 300 and 600°C (Fig. 4).

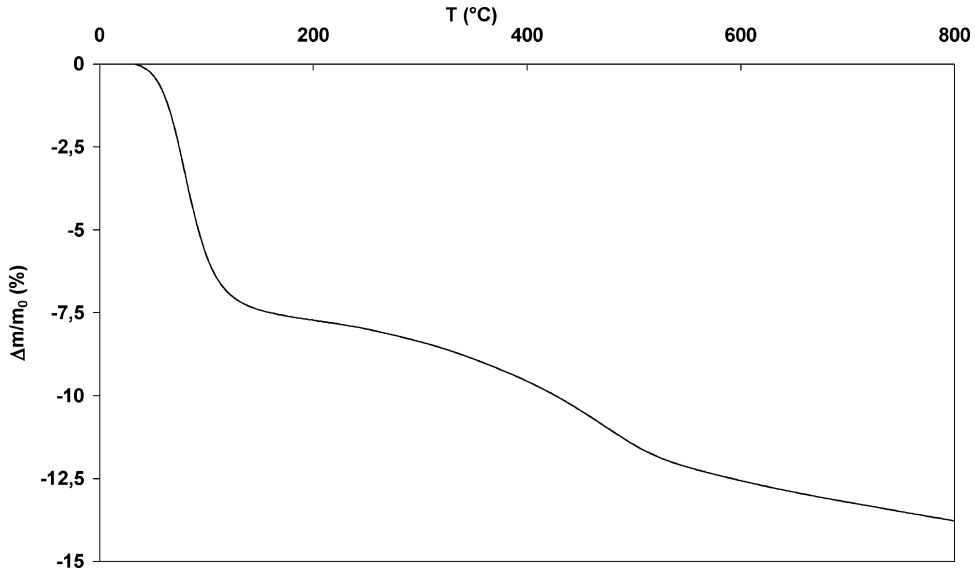

Figure 4. TGA curve for sample SZ4-B (heating rate = 5°C/min).

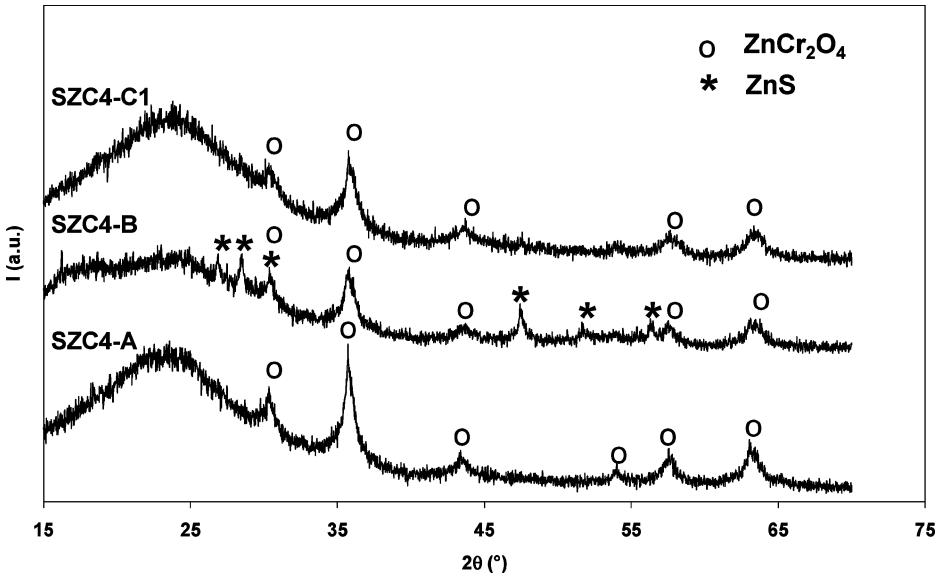

Figure 5. X-ray patterns for different samples SZC4.

The dehydroxylation of the silanols groups which occurs in the same range of temperature [13] hinders the gravimetric quantification of the yield of zinc sulfurization.

In the case of powder SCZ4-A, the X-ray pattern (Fig. 5) shows the presence of broad peaks which can be assigned to nanocrystallites of spinel $ZnCr_2O_4$ [14]. After treatment under H_2S (sample SZC4-B), diffraction peaks of ZnS appear on the corresponding pattern (Fig. 5). No peak related to $ZnCr_2S_4$ can be detected but a decrease of the relative intensity of the peaks of $ZnCr_2O_4$ is observed. It can be deduced that germination and growth of ZnS would occur at the expense of the $ZnCr_2O_4$ phase. After treatment under air at 500°C for 90 min (sample SZ4-C1), the X-ray pattern is similar to that of the starting material (Fig. 5). As in the previous case, the experimental results indicate the reversibility of the chemisorption of H_2S as ZnS.

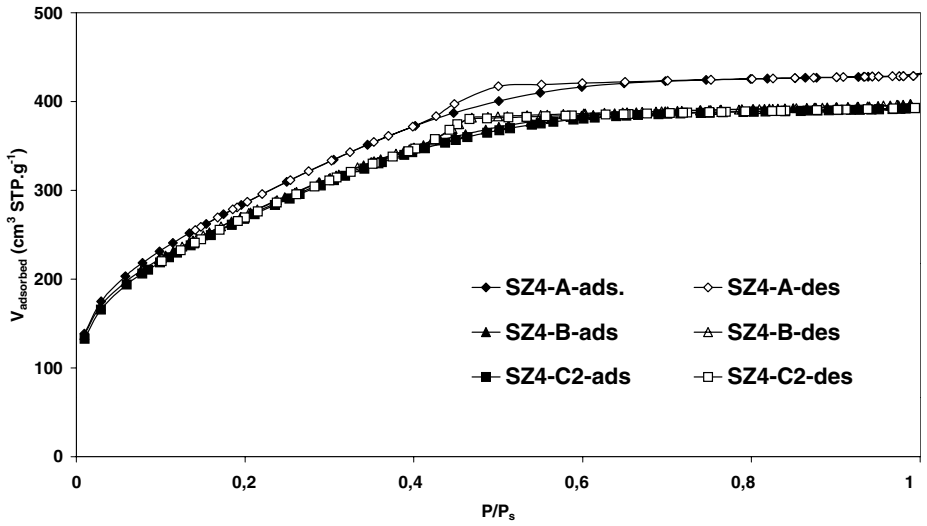

Figure 6. N_2 adsorption-desorption isotherms for different samples SZ4.

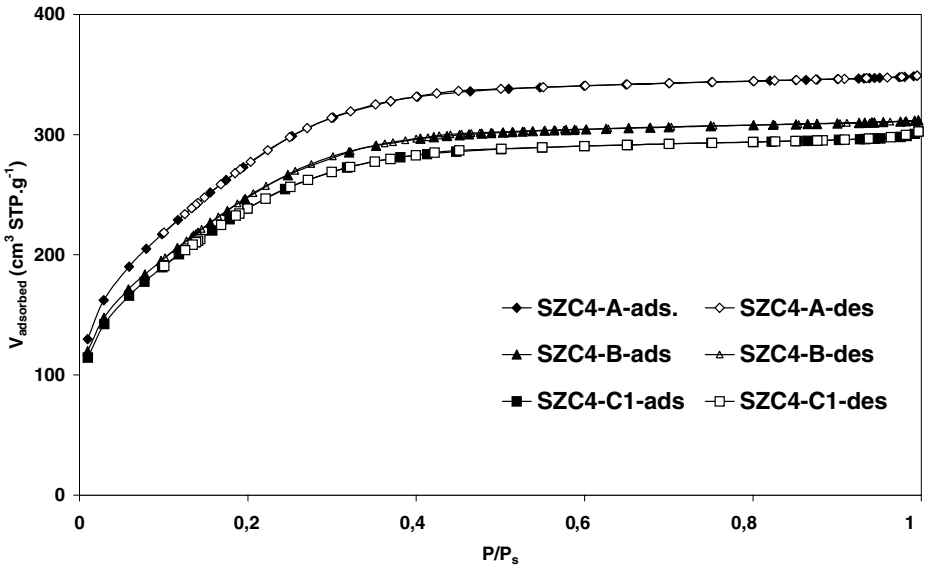

Figure 7. N_2 adsorption-desorption isotherms for different samples SZC4.

3.3. Evolution of the Porosity

Different nitrogen adsorption-desorption isotherms and main porosity characteristics are reported in Figs. 6 and 7, and Table 1, respectively. For powder SZ4-A, the isotherm curve reported in Fig. 6 can be defined as type I using the IUPAC classification [7] despite the presence of a very small hysteresis loop at low relative pressure. A type I isotherm is associated with a microporous material whereas the hysteresis loop is usually related to capillary condensation in mesopores. The mean pore size which is equal to 2.5 nm (Table 1) is actually located at the boundary value between the micropores and the mesopores which is 2 nm. The MP pore size analysis indicates that all the hydraulic radii are less that 1 nm. Assuming cylindrical pores, the upper limit of equivalent diameter is thus equal to 4 nm. High specific surface area and porosity were measured,

Table 1. Porosity characteristics for different samples.

Sample	Specific surface area, S_{BET} ($m^2 \cdot g^{-1}$)	Porosity (%)	Mean pore size, d_p (nm)
SZ4-A	1060	59	2.5
SZ4-B	1000	57	2.4
SZ4-C2	1000	57	2.4
SZC4-A	1050	54	2.1
SZC4-B	940	51	2.1
SZC4-C1	900	50	2.1

1060 $m^2 \cdot g^{-1}$ and 59%, respectively. After successive long thermal treatments at 500°C under H_2S and then under air (samples SZ4-B and SZ4-C2), a very low decrease of the main porous texture parameters is observed compared to the values measured on the initial sample heat treated for only 45 min at 550°C (Table 1). It can be concluded that the synthesized nanoporous material exhibits a good thermal stability in this range of temperature.

For powder SCZ4-A, the isotherm curve is strictly of type I (Fig. 7) with no more hysteresis loop. A lower mean pore size (2.1 nm) is determined in agreement with the disappearance of the hysteresis loop due to the capillary condensation in the largest pores of samples SZ4. The good thermal stability of the porous texture is also observed for samples SZC4 (Fig. 7 and Table 1). The lower mean pore size value for samples SZC4 can be explained taking into account the effect of the Zn_{II} and Cr_{III} salts on the acidity of the starting solutions of TEOS. It is well known that a more basic sol favors the formation of larger pores [13]. In our study, the cation Cr_{III} is more acidic than the cation Zn_{II}. An experimental evidence of this property was obtained with the preparation of aqueous solutions with same salt concentrations as the ethanolic TEOS solutions. The pH measured for the "$ZnCr_2$" aqueous solution was equal to 2 whereas the pH was equal to 6 in the case of the "Zn" solution. After successive additions of acidic and basic water, the final pH values were 3 and 7 for the "$ZnCr_2$" and "Zn" solutions, respectively.

The synthesized materials exhibit attractive porous characteristics with regard to the considered application: a high specific surface area and a low pore size in order to favor an efficient H_2S chemisorption, a high porosity to promote a good gas permeability of the nanofilters. These porous characteristics can be still optimized by modifying the acid-base conditions of the silica polymerization and also the content of organic additive. As a matter of fact, it was previously shown that the decrease of the Si/X45 molar ratio induces a significant increase of the porosity without important change of the mean pore size [6].

4. Conclusion

Nanoporous silica powders and coatings containing active oxide dispersions have been synthesized by the sol-gel route. As a function of the sol formulation, composite membranes or supported thin layers can be prepared on porous ceramic substrates. Experiments of H_2S chemisorption evidenced the activity and the regenerability of the two types of nanocomposite materials containing ZnO and $ZnCr_2O_4$, respectively. These materials exhibit nanometric pores, high surface area and high porosity. These porous characteristics are maintained after successive treatments of H_2S chemisorption and regeneration under air.

These preliminary results encourage to pursue this study which aims at the preparation of nanofilters dedicated to the retention of hydrogen sulfide by chemisorption in gas mixtures. Optimization of the synthesis conditions is now required. An increase of the content of active oxide without significant change of the porous characteristics of the prepared materials would be particularly attractive. Moreover permeation measurements have to be performed to validate the adsorption efficiency of the prepared filters. On the other hand, it must be noted that nanoporous coatings containing $ZnCr_2O_4$ nanocrystallites could be interesting for the development of catalytic membranes for the direct synthesis of alcohols [17, 18].

Acknowledgments

The authors thank Prof. R. Fourcade (LAMMI/ University Montpellier II) for helpful discussions.

References

1. J.B. Gibson III and D.P. Harrison, Ind. Eng. Chem. Process Des. Dev. **19**, 231 (1980).
2. P.J.H. Carnell, in *Catalyst Handbook*, 2nd edn., edited by M.V. Twigg (Wolfe Publishing Ltd, London, 1989), p. 191.
3. T. Baird, K.C. Campbell, P.J. Holliman, R. Hoyle, D. Stirling, and B.P. Williams, J. Chem. Soc. Faraday Trans. **91**, 3219 (1995).
4. R.L. Goswamee, A. Ayral, K.G. Bhattacharyya, and D.K. Dutta, Materials Letters **46**, 105 (2000).
5. A.J. Burggraaf and L. Cot (eds.), *Fundamentals of Inorganic Membrane Science and Technology* (Elsevier, Amsterdam, 1996).

6. A. Ayral, C. Balzer, T. Dabadie, C. Guizard, and A. Julbe, Catalysis Today **25**, 219 (1995).
7. S. Lowell and J.E. Shields, *Powder Surface Area and Porosity* (Chapman & Hall, London, 1984).
8. A. Tamditi, Thesis, Montpellier (France) 1995.
9. R.A. Nyquist and R.O. Kagel, *Infrared Spectra of Inorganic Compounds* (Academic Press, New York, 1971).
10. Joint Committee on Powder Diffraction Standards, Powder Diffraction File, Card Nr. 14–0653.
11. E.N. Bunting, J. Am. Ceram. Soc. **13**, 8 (1930).
12. Joint Committee on Powder Diffraction Standards, Powder Diffraction File, Card Nr. 79-2204.
13. C.J. Brinker and G.W. Scherer, *Sol-Gel Science, the Physics and Chemistry of Sol-Gel Processing* (Academic Press, San Diego, 1990).
14. Joint Committee on Powder Diffraction Standards, Powder Diffraction File, Card Nr. 73-1962.
15. W.R. Moser and K.E. Connolly, The Chemical Engineering Journal **64**, 239 (1996).
16. G.W. Roberts, M.A. Marquez, and M. Shawn McCutchen, Catalysis Today **36**, 255 (1997).
17. G.W. Roberts, M.A. Marquez, and C.A. Haney, Applied Catalysis A: General **183**, 395 (1999).
18. X. Sun, N.W. Jones, J.C. Gesick, L. Xu, and G.W. Roberts, Applied Catalysis A: General **231**, 269 (2002).